Sustainable Energy Technologies and Assessments 83 (2025) 104541

Contents lists available at ScienceDirect

Sustainable Energy Technologies and Assessments

journal homepage: www.elsevier.com/locate/seta

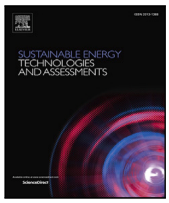

Original article

Integrated adequacy and stability BESS sizing criteria for hybrid diesel–PV microgrids in developing countries

Corrado Maria Caminiti [a,*], Matteo Spiller [a], Aleksandar Dimovski [a], Jacopo Barbieri [b], Enrico Ragaini [c], Marco Merlo [a]

[a] Department of Energy, Politecnico di Milano, 20156 Milano, Italy
[b] St. Mary's Hospital Lacor, Uganda
[c] ABB, Dalmine, Italy

ARTICLE INFO

Keywords:
Multipurpose battery sizing
Microgrid
Genetic algorithm
Transient stability analysis
Developing countries

ABSTRACT

In rural areas of developing countries, microgrids paired with energy storage offer a reliable, decentralized solution to electrification, enabling the continuous supply of power and the integration of renewable energy sources despite fluctuations in generation during peak demand. The present work proposes a novel, real-life measurement-based, holistic methodology to support multipurpose battery sizing in grid-connected microgrids, including adequacy and stability considerations within a single sizing process. In terms of energy, a numerical sizing procedure is applied to a yearly, hourly discretized load demand profile for primary energy. Subsequently, the system's dynamic response characterization relies on a multi-offspring genetic algorithm to tune a high-fidelity governor. A transient stability analysis is performed to determine the additional power required to ensure stable service provision. The proposed procedure is applied to the microgrid of St. Mary's Hospital Lacor in Uganda, addressing the challenges of grid instability and the need for curtailment in PV-based systems in a real-life scenario. The final sizing analysis showed that a limited size battery is effective in reducing yearly curtailment by 42.9%, limiting frequency peak-to-peak fluctuations by 64.1%.

Introduction

Given the urgent need to accelerate the pace and broaden the geographic reach of the energy transition, along with harnessing its complete potential in attaining socio-economic development objectives, there is a pressing demand for innovative solutions. These instruments should assist developing countries in realizing the long-term advantages of the energy transition without exacerbating the fiscal constraints of their economies [1]. Nevertheless, in regions like Sub-Saharan Africa where 80% of the global population lacking electricity reside, access to electricity remains a significant impediment to socio-economic advancement. Microgrids (MGs), clusters of consumers, storage devices, and distributed generators that may be connected to the network, represent an established and effective solution for last mile communities [2].

Sizing MG's assets, especially in rural areas, is inherently complex due to the need to synchronize unpredictable energy sources with uncertain load demands, ultimately striving to ensure optimal reliability and cost-effectiveness. Depending on the MG's features, multiple considerations are possible in the design stage. Firstly, the location and electricity demand of the system represent pivotal information for the nominal sizing of the assets. Moreover, parameters such as solar irradiance, ambient temperature, wind velocity, and relative humidity enable a reliable forecast of non-dispatchable PV generation by providing valuable insights into the photovoltaic (PV) system's performance [3]. Secondly, depending on the type of MG and the criticality of the load served, technical and reliability considerations gain importance, especially regarding the capability to fulfill demand under specific circumstances, such as the unavailability of the main grid [4]. In this regard, network-electrified communities and interconnected MGs face reliability challenges due to the limitations of the existing infrastructure. This poses an additional risk, particularly for critical loads. Felice et al. in [5] illustrate that mitigating this risk is often achieved through backup Diesel Generators (DGs), which significantly increase greenhouse gas emissions and energy provision costs. In contrast, a more sustainable alternative that incorporates additional PV systems with batteries offers superior emission reduction, lower energy costs, and enhanced reliability [6].

* Corresponding author.
E-mail addresses: corradomaria.caminiti@polimi.it (C.M. Caminiti), matteospiller@polimi.it (M. Spiller), aleksandar.dimovski@polimi.it (A. Dimovski), barbieri.jacopo@lacorhospital.org (J. Barbieri), enrico.ragaini@it.abb.com (E. Ragaini), marcomerlo@polimi.it (M. Merlo).

https://doi.org/10.1016/j.seta.2025.104541
Received 22 December 2024; Received in revised form 18 August 2025; Accepted 23 August 2025

In this framework, Battery Energy Storage Systems (BESSs) are indispensable components increasing the penetration of intermittent energy sources, enhancing system adequacy, providing a reliable backup source, and improving power quality by alleviating frequency and voltage oscillations [7]. Despite their crucial role, there is a noticeable absence of a comprehensive BESS sizing methodology that addresses the diverse needs of different applications. Energy-oriented methodologies for BESS sizing in PV-centered MG systems are categorized by Tamer et al. [8]. Intuitive methods, relying on average meteorological data, often lead to improper sizing and higher costs due to oversimplification. Numerical methods provide more detail but yield sub-optimal solutions due to linear decision-variable changes. Analytical methods lack flexibility, while software tools are limited in refining components and specifications, failing to address key rural electrification factors, such as load uncertainties and demand evolution. At the same time, batteries contribute to frequency regulation in systems with high deployment of Renewable Energy Sources (RES). Intermittent generation and load patterns, exacerbated by low inertia systems and the rising penetration of RES, can significantly impact the MG's normal operation. Moreover, the switch from grid-tied to standalone mode of operation, combined with low rotating inertia are among the main causes of power imbalance and voltage fluctuations [9]. Authors in [10] propose a frequency stability-constrained battery energy storage system within a Mixed Integer Linear Programming (MILP) formulation relying on Bender's decomposition. The transient dynamics are included considering a time-domain model based on the discretized swing equation. In [11], a meta-heuristic optimization procedure was developed to optimally size a BESS system to support frequency control in an islanded MG in Australia. Using DIGSILENT PowerFactory, the transient frequency deviation under the power system critical contingencies was tested. The BESS was proven to be essential in supporting frequency control, closely linked to the maximum admitted RES penetration.

To properly analyze and model the system's dynamic response, a high-frequency measurement campaign would be required, alongside accurate modeling of the regulators present in the MG. Specifically, in DG-based MGs, governor parameters are essential input. Generally, the role of a DG's speed governor is to regulate the engine speed by adjusting the fuel intake; increasing the fuel rate boosts the mechanical power applied to the shaft while decreasing it reduces the power [12]. The significance of a high-fidelity governor-engine model becomes clear in various aspects: in [13], the necessity for a dependable model of the diesel-powered MG on Kinmen Island is highlighted, particularly for conducting stability and contingency analyses. Parameters are tuned and validated using field data employing hybrid particle swarm optimization. A similar approach, aimed at identifying and tuning parameters for the governor model structure is proposed in [14]: four alternative control logic are compared and tuned concerning the field data recorded by the Alaska Center for Energy and Power in an isolated MG for a 400 kVA DG. The set of unknown parameters is estimated as minimizing a multiobjective function, whose terms correspond to the weighted sum of the errors between the measured and simulated response of active and reactive power, voltage, and frequency. DG parameters are estimated by employing an iterative procedure in MATLAB. Field experimental data are derived from an ad hoc experimental setup: load steps of 240 kW and 160 kVAR are imposed on the system, previously operating with a stationary load of 80 kW and 0 kVAR and response is recorded consequently. Likewise, Zaker et al. in [15] propose a methodology for characterizing model parameters in a grid-connected MG based on a Genetic Algorithm (GA). The tuning procedure relies on measurements of active and reactive power exchanges at the point of common coupling. A nonlinear seventh-order synchronous machine is considered to represent the DGs. Simulations are carried out relying on iterative interactions between MATLAB and DIGSILENT Power Factory software.

Integrated multipurpose BESS sizing methodologies and high-fidelity parameter tuning in generator governors are two well-established aspects of MGs. However, there is a notable lack of research that adopts a systemic approach capable of specifically assessing the battery sizing problem employing a data-driven characterization of the dynamic response of conventional rotating machines. Addressing this issue is increasingly relevant due to the technological maturity of BESS and the necessity to integrate them into existing systems. This need is even more critical in developing countries, where improvements can have a higher incremental benefit for the local population and where the operational framework often faces data scarcity. In particular, this problem impacts both the samples related to the load and generation power profile and the setup of the automatic controls in place, such as the automatic generator control's parameters and voltage regulators. Despite being recognized as a technical challenge affecting microgrids in developing countries [16], the optimal sizing of BESS systems is mainly driven by economic criteria performed on simplified energy models, typically solely evaluating the steady state operation of the MG, to minimize the expected net present cost of the system, accounting for the investment costs (CAPEX), the average operational expenses (OPEX) and the economic value of the unserved energy [17]. Moreover, the temporal discretization step is based on hourly intervals, ignoring load and generation fluctuations that may occur on shorter timescales during both the design and subsequent validation phases, leading to a partial comprehension of the system [18,19].

Hence, this study aims to bridge this gap by proposing a holistic BESS sizing methodology for RES-based grid-connected MGs in developing countries. The methodology utilizes a limited measurement campaign to gather essential data on load characteristics and assess the system's transient response, optimizing the DG governor through a real-coded genetic algorithm. A multipurpose BESS sizing approach is introduced, initially addressing adequacy requirements using hourly discretized consumption and generation data. The scope is then expanded through transient stability analysis, potentially leading to an incremental increase in storage capacity, both in energy and power, to enhance stability. The main contribution of this study lies in providing a practical and adaptable BESS sizing framework that integrates both adequacy and transient stability requirements, specifically tailored for data-scarce developing regions.

The remainder of this paper is structured as follows: Section "Materials and Methods" outlines the methodology, detailing the mathematical formulation for optimal power dispatch, genetic tuning, and stability sizing. Section "A real-life case study: the Lacor Hospital" introduces the case study and numerical assumptions, while Section "Result and Discussion" presents the simulation results, culminating in the integrated optimal BESS sizing. Finally, Section "Conclusions" concludes the study by summarizing the key insights and suggesting directions for future research.

Materials and methods

The main objective of the proposed procedure is to examine an existing grid-connected, diesel-based MG aiming at integrating incremental production by renewable generators. In MG operations, it is crucial to evaluate technical constraints: nearing the hosting capacity limit, several problems could arise, including severe frequency stability degradation, undervoltages, excessive line losses, overloading of transformers and feeders, and protection failures [20]. An overview of the potential operational conditions and the associated challenges the system may encounter is presented in Table 1.

In order to properly model those phenomena, detailed models of the MG generation portfolio and of the load should be developed. Given the focus on developing countries, where data availability is often limited, this paper proposes a methodology designed to work with minimal data from the field. Therefore, the article proposes a new data-driven approach designed to be easily replicable. The model relies on the acquisition of electrical frequency samples correlated with the operational load of the MG, even if only for limited time intervals, using portable measuring instruments. Owing to this dataset, a GA is

Table 1
MG supply configurations.

Configurations	Operational constraints	Objective
Grid-tied	–	–
Grid-tied + PV	No injection	Minimize solar curtailment
Stand-alone - DG	Low inertia, ramp limit	Limit frequency fluctuations
Stand-alone - DG + PV	Low inertia, ramp limit and no injection	Limit frequency fluctuations and minimize solar curtailment
Stand-alone - DG + PV + BESS	–	Optimal dispatch of the DG and maximize PV production

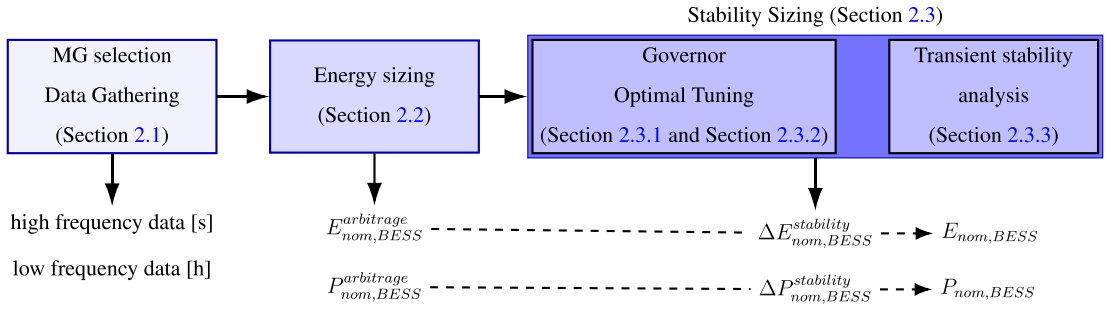

Fig. 1. Holistic MGs sizing key steps.

proposed to estimate the parameters of the dynamic model of the DG. Finally, the digital twin of the MG is exploited to design the BESS equipment properly. From the broadest perspective, the work comprises three principal, hierarchically ordered, steps, as illustrated in Fig. 1.

Data gathering and data processing

Data scarcity often limits the quality and the scope of analysis [21]. This challenge is particularly pronounced in developing regions, where measurements' accuracy and reliability are limited. In the approach proposed in this paper, the input dataset has been limited to a subset of information that is supposed to be commonly available:

- The hourly discretized electric load P_t^{load} and source of the supply (Solar PV P_t^{PV}, DG P_t^{DG} or national grid P_t^{grid}) records for an adequate time-window, e.g. a year.
- High temporal resolution measurements for the electric net demand d_t and frequency f_t are necessary for stability-oriented sizing. These data are supposed to be gathered with mobile equipment, i.e. are supposed to be available only for limited time intervals (corresponding to a focused measurement campaign), moreover, the sampling frequency is limited to 1 Hz. For each notable quantity, maximum, minimum, and mean measurements are recorded over the sampling period.

Hourly discretized records are employed in the energy sizing of the BESS. On the other hand, as stated in [22], frequency fluctuations, analytically regulated by the swing equation reported in Eq. (1), represent the response to power imbalances in power systems:

$$M_{DG}\frac{d\omega}{dt} + D_{DG}\Delta\omega = P_m - P_l \tag{1}$$

where the mechanical input power, the electrical output power, the angular velocity of the rotor, the inertia and damping coefficients of the DG are respectively P_m, P_l, ω, M_{DG} and D_{DG}.

Stability-wise, islanded MGs are considered low-inertia systems. These systems may experience significant frequency perturbations in response to sudden load changes or faults. As a result, an efficient approach to identify stand-alone configuration is to monitor the frequency deviation, Δf_t, and the Rate of Change of Frequency, $RoCoF_t$, ensuring they remain within stability thresholds ($\Delta\hat{f}_t$ and $\hat{RoCoF}$). Here, the frequency deviation at time t, Δf_t, is defined as the difference between the maximum and minimum frequency values measured over the sampling period, i.e., $f_t^{\max}$ and $f_t^{\min}$, respectively. Applying Eqs. (2) and (3), coupled with a forward-moving average scanning procedure, off-grid segments can be isolated from the frequency measurements.

$$\Delta f_t = f_t^{\max} - f_t^{\min} \geq \Delta\hat{f}_t \tag{2}$$

$$RoCoF_t \geq \hat{RoCoF} \tag{3}$$

During stand-alone operations, BESS is a viable solution to mitigate the extent of oscillations and support the energy balance of the system. For this reason, once the hourly energy status of the MG is available over a long time window, i.e. one year, and detailed data have been gathered at least over a limited time window (a few reference hours), it is possible to approach the BESS design. As previously pointed out, this is split into two steps: energy sizing and stability sizing.

Energy sizing of the BESS

As anticipated in Section "Introduction", energy-based sizing methodologies have been widely investigated in literature resulting in several parallel valid approaches. Limiting the scope to medium to large MGs, with power peaks higher than several hundred kilowatts, achieving a net-zero solution, phasing out fossil-based generators, is impractical due to factors such as load magnitude, reliability requirements, and investment constraints. Nonetheless, an effective steady state methodology is here proposed in order to exploit limited size battery in mitigating renewable curtailment and improving security of the supply in the transition to off-grid operations.

A numerical, economic oriented, rule-based dispatch logic is developed to evaluate BESS's adequacy to the load and renewable profile. As reported in Algorithm 1, the control logic prioritizes energy from the grid to supply the net load, whereas it gives priority to the BESS over the DG during off-grid operations. On the other hand, charging of the BESS will only take place in presence of PV over-generation.

At the heart of this evaluation are the nominal capabilities of the BESS, $E_{nom,BESS}$ and $P_{nom,BESS}$, in Eq. (4), which significantly impact the Net Present Value (NPV) of the investment, as shown in Eq. (5). The capital expenditure $CAPEX_{BESS}$ is expressed as:

$$CAPEX_{BESS} = \hat{C}\cdot E_{nom,BESS} + \hat{P}\cdot P_{nom,BESS} \tag{4}$$

where $\hat{C}$ and $\hat{P}$ represent the specific investment costs per unit of energy capacity ($/kWh) and power capacity ($/kW), respectively.

The NPV formulation incorporates both the initial investment and the discounted operational costs:

$$NPV = CAPEX_{BESS} + \sum_{y \in \overline{Y}} \frac{O\&M^{y}_{DG} + F^{y}_{DG} + IC^{y}}{(1+r)^{y}} \quad (5)$$

The trade-off condition arises from the reduction in operational and fuel costs of the DG, $O\&M^{y}_{DG}$ and F^{y}_{DG}, along with the interruption cost IC^{y}, which accounts for reliability improvements by quantifying the fraction of net demand bridged in the hour following a blackout event. Steady-state, hourly discretized power balances are performed over a full year of operation and assumed identical over the investment lifetime $\overline{Y}$. r denotes the discount rate, reflecting the time value of money.

Stability constraints in sizing the BESS

Considering the importance of stability in MG operation, an additional step is necessary to fully characterize the system and enhance the robustness of the sizing procedure.

As anticipated in Fig. 1, the current section of the methodology can be broken down into two subsequent steps. Firstly, developing a digital twin model of the system is indispensable for conducting transient stability analysis. Specifically, the DG controller parameters, which are responsible for the dynamic response of the MG, must be properly tuned to accurately assess the frequency deviations caused by load transients. Therefore, Sections "Genetic Algorithm-Based Tuning for DG Governor Characterization" and "Iterative Tuning for Converging Parameter Estimations" are devoted respectively to the theoretical presentation of the GA employed for the optimal tuning and its configuration within the framework of various isolated off-grid observations. This process involves the use of multiple high-frequency measurements isolated in Section "Data Gathering and Data Processing". By utilizing the electric load and recorded frequency data, dynamic simulations are performed in DIGSILENT software, comparing the simulated behavior with the measured one, albeit for limited periods. Once the dynamic constants regulating transients within the system are fully characterized, a BESS can be added to the dynamic model and load transients simulated. Stability sizing is completed when the simulated frequency response meets predefined stability and power quality criteria (Section "Dynamic Simulation of BESS for Fast Frequency Response").

Genetic algorithm-based tuning for DG governor characterization

An indispensable preliminary stage, crucial for the overall sizing process, entails the precise characterization of the DG. With respect to measurements, in developing countries where old DGs are typically employed, speed governors' characterization is often missing or inaccurate [23].

For this reason, a GA is designed to optimize the DG governor's parameters, ensuring a high-fidelity dynamic response of the system. A flowchart of the procedure is presented in Fig. 3, where tasks performed using Python and DIGSILENT are highlighted with green and blue backgrounds, respectively. The objective of the GA is to explore the search space, adjusting parameters to minimize the discrepancy between the simulated frequency response and the measured data. The Woodward governor DEGOV1, a well-established and widely used model in the literature [13,24], was adopted as the control architecture. Once the governor model is selected, the parameters within the control blocks of Fig. 2a, along with the inertia constant J, constitute the complete set of control variables available for optimal tuning. In Fig. 2a, w_{ref}, w, P_{elec}, and P_{mech} represent the angular reference speed, angular speed, electrical power of the generator, and the output torque of the machine, respectively. Since this study focuses on the active power sizing of the BESS, the investigation of the exciter and power system stabilizers is beyond its scope.

The GA model adopted is a multi-offspring improved real-coded genetic algorithm described in [25]. It exploits a HNDDBX to identify the parameters that best fit the objective function. This strategy guarantees that the cross-generation of the offspring is closely located in the fittest sample of the previous generation. Secondly, a combined mutation method is proposed to achieve both local and global search to avoid the shortcomings of a single mutation. The combinatorial mutation changes the mutation type in every iteration of the GA. The mutation techniques adopted are Cauchy distribution, normal distribution, and Levy fight.

The tuning of governor parameters had as an objective function the coefficient of determination R^2 between the samples gathered from the field and the ones generated in DIGSILENT. The data obtained from the simulation undergo processing to adapt the sampling period of simulations to the one-second sampling period of the real energy meter. The post-processing of the transient simulation output to one second exploits the mean of the value within the resampling interval. Moreover, the objective function also includes a penalty factor based on the Fourier transform to avoid an unstable outcome. Indeed, with weak damping and oscillations, the system could become unstable [26]. Since oscillations increase, a frequency signal with a high-order harmonic content is produced. Therefore, the signal obtained from every simulation is processed with the Fourier transform, and harmonic content above 20 Hz is penalized. This approach allows for the discarding of parameters that lead to poor damping or instability during transient. Eq. (6) describes the objective function to minimize:

$$R^2 + c \cdot F^{penalty} = 1 - \frac{\left(freq^{resampled}_{DIGSILENT} - freq_{real}\right)^2}{\left(freq^{resampled}_{DIGSILENT} - \bar{freq}_{DIGSILENT}\right)^2} + c \cdot F^{penalty} \quad (6)$$

$$F^{penalty} = \begin{cases} 0 & \text{if } f \leq 20 \text{ Hz} \\ \sum armonic\ content^{f \geq 20 \text{ Hz}} & \text{if } f \geq 20 \text{ Hz} \end{cases} \quad (7)$$

where R^2 represents the coefficient of determination, $freq^{resampled}_{DIGSILENT}$ is the frequency simulated, $freq_{real}$ the measured value and $\bar{freq}_{DIGSILENT}$ the simulated averaged value. In addition, c is a weight parameter for the Fourier penalty function $F^{penalty}$ that is evaluated as in Eq. (7). The crossover of the parents into offspring takes the best samples identified by the objective function. Lastly, mutation modifies the offspring with a probability based on the current iteration. The mutation probability is inversely proportional to the square root of the iterations. This value allows exhaustive research of the variable space at the beginning of the algorithm. The type of mutation changes in the function of the iteration. Specifically, the first iteration exploits the Cauchy distribution, the second iteration adopts the normal distribution, and the third iteration applies Levy flight. Subsequently, the fourth iteration uses the Cauchy distribution again, and this pattern continues in a cyclic manner. Once the algorithm generates the offspring, a new iteration starts. The convergence criteria for the algorithm is the number of iterations. Algorithm 2 summarizes all the steps of the developed evolutionary algorithm.

Iterative tuning for converging parameter estimations

Given the multitude of governor parameters to be estimated and the number of off-grid periods recorded, an iterative procedure is developed. The optimal set of parameters is extracted recurring to the procedure presented in Section "Genetic Algorithm-Based Tuning for DG Governor Characterization". Optimal search may not result in the same numerical values for each instance. For this reason, at each iteration, those parameters that have a clear and shared value among all the different records are kept valid and removed from optimal search. This was developed starting from the idea that genetic search was here employed given the high number of uncertain parameters and, detached from the physical nature of the problem, could lead to an acceptable solution yet not in line with the real-life operation of the machine. The termination criterion for a parameter can be reached either through Eq. (8), which utilizes the coefficient of variation CV,

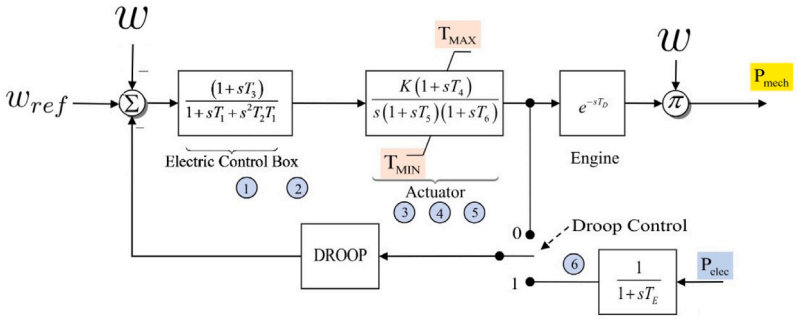

(a)

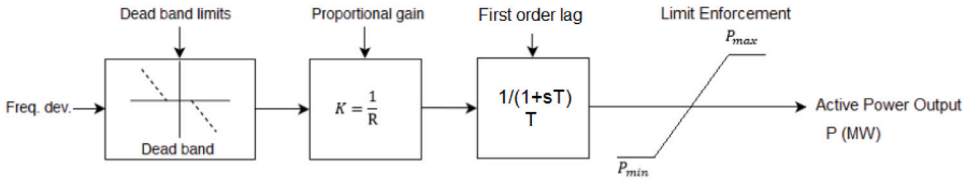

(b)

Fig. 2. (a) DEGOV1 governor model and (b) Block diagram implemented for BESS frequency control.

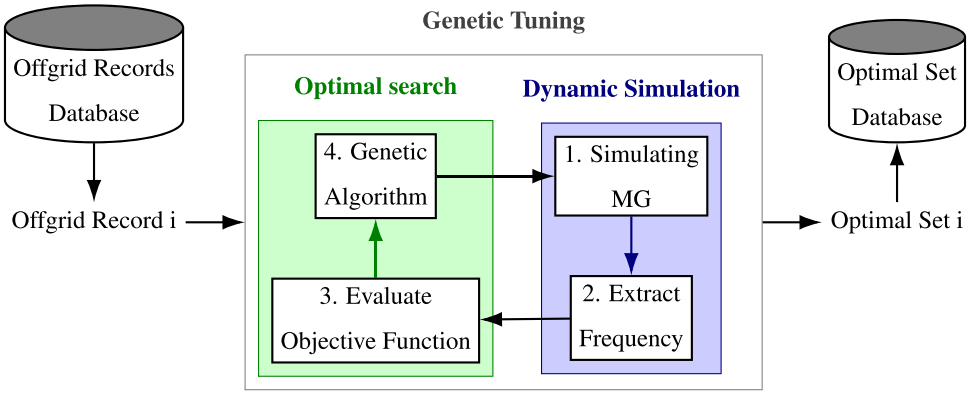

Fig. 3. Genetic tuning of DG governor's parameters. (For interpretation of the references to color in this figure legend, the reader is referred to the web version of this article.)

or by establishing a clear correlation with zero. Eq. (8) is quantifying the dispersion of the N parameters' estimation x_i with respect to the average $\bar{x}$. In other words, the exit condition can also be met when a considerable number of samples indicate that a particular parameter lacks significance in characterizing the response.

$$CV = \frac{\sqrt{\frac{\sum(x_i-\bar{x})^2}{N}}}{\frac{\sum x_i}{N}} \cdot 100 \tag{8}$$

Additionally, referring to the schematic in Fig. 2a, throttle feedback loop time constant te can be implicitly disabled by the switch position and converge to optimal values detached from the real dynamic response as it is not impacting in the DG's behavior. Progressively a greater number of parameters are freezed and fixed to the agreed optimal value enabling in-depth investigation of those parameters that embeds most of the variability. To isolate the impact of each subsequent parameter selection, termination criterion involves only one parameter per each iteration. The entire procedure is summarized in Fig. 4.

Dynamic simulation of BESS for fast frequency response

With a fully characterized system's dynamic response, proper transient stability analysis of the MG can be performed. Clearly, for the MG under investigation, the user of the tool is required to specify the maximum allowable frequency fluctuation and iteratively adjust

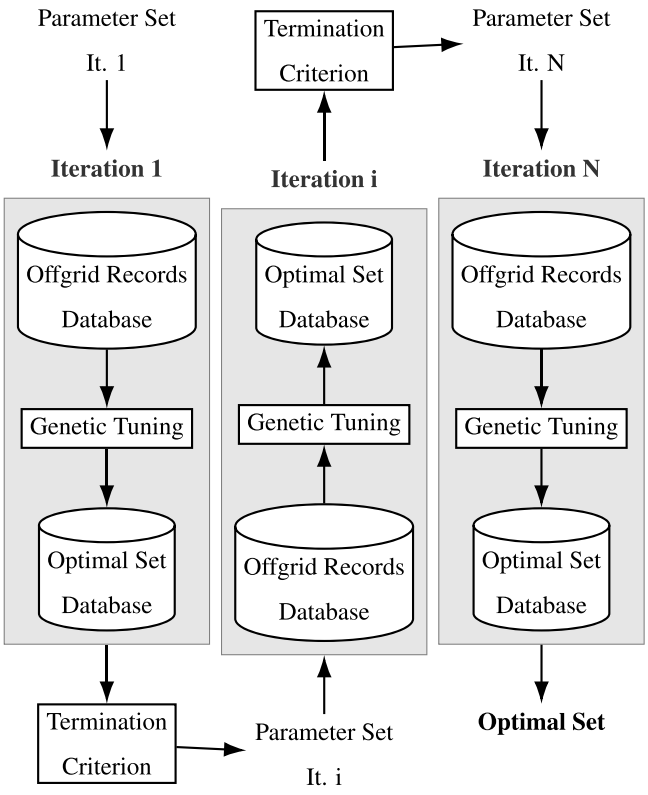

Fig. 4. Iterative procedure flowchart.

Table 2
Numerical economical assumptions.

$\hat{C}$ [€/kWh]	$\hat{P}$ [€/kW]	$OPEX_{DG}$ [€/h]	F_{DG} [€/L]	r [%]
205	82	1,7	1,3	6

the simulations by increasing the nominal power of the BESS until the target performance criteria are met. Finally, the results of the simulation will yield data on the energy charged or discharged by the BESS, enabling the quantification of the BESS capacity allocated for Primary Frequency Control (PFC). PFC is a control strategy aimed at containing system frequency deviation, reducing nadir and RoCoF during transient.

A BESS is included in the DIGSILENT PowerFactory model of the MG. Transient analysis results in a simulated frequency profile. The model emulates the behavior of traditional frequency containment reserve control, with three parameters: deadband, droop and control delay. Proportional controller with a dead band is implemented and the droop curve is regulated by Eq. (9):

$$K_p = \frac{\frac{\Delta f}{f_{nom}}}{\frac{\Delta P_e}{P_{eff}}} \tag{9}$$

where ΔP_e is the power set point of the frequency regulation, $\frac{\Delta f}{f_{nom}}$ the frequency deviation in p.u. and P_{eff} the BESS nominal power. A representation of the block diagram is reported in Fig. 2b. Droop-controlled BESS, especially in small isolated systems, are demonstrated to directly enhance operation reliability and quality of the supply [27,28]. A detailed description of the BESS model, comprehensive of charging and discharging efficiency, capability curves and fade out duration of the model is proposed in [29].

Integrated sizing

The final step of the procedure is devoted to the final optimal sizing. Complementary information deriving from the energy and stability oriented sizing are combined at this point.

To secure operations of the off-grid system, a coincidence factor CF must be introduced. Given the two different time granularity of simulations, it is relevant to state that power demand may not occur simultaneously, suggesting the risk of a possible overestimation of power capability needs. Coincidence factor estimating the likelihood of the superposition of the frequency control service over the BESS energy provision is introduced for this reason. From an energy perspective, allocating additional capacity is application specific. Reliability requirements for energy provision purposes may justify an increment of the BESS nominal size. Analytically the approach is formalized in Eqs. (10) and (11):

$$E_{nom,BESS} = E^{arbitrage}_{nom,BESS} + \Delta E^{stability}_{nom,BESS} \tag{10}$$

$$P_{nom,BESS} = P^{arbitrage}_{nom,BESS} + CF \cdot \Delta P^{stability}_{nom,BESS} \tag{11}$$

where the integrated sizing, $E_{nom,BESS}$ and $P_{nom,BESS}$,is obtained by combining the energy and power requirements from Section "Energy Sizing of the BESS", which define the arbitrage-related components ($E^{arbitrage}_{nom,BESS}$, $P^{arbitrage}_{nom,BESS}$), and Section "Stability constraints in sizing the BESS", which account for the additional capacity needed to ensure stability ($\Delta E^{stability}_{nom,BESS}$, $\Delta P^{stability}_{nom,BESS}$).

A real-life case study: the Lacor Hospital

To test and validate the proposed methodology, a case study was conducted at St. Mary's Hospital Lacor in Uganda, one of the largest private non-profit institutions in Sub-Saharan Africa [30]. Electricity-wise, it is operated as a grid-connected MG; 1 MVA transformer represents the interface to an 11 kV feeder operated by UMEME, the national grid operator. Physical assets of the MG consist of a solar power plant of 335 kW of nominal power while conventional inertia is ensured by DGs. Over-sizing of the controllable assets is induced by the presence of critical medical loads that must not be interrupted under any circumstances. Moreover, due to the grid's high unreliability, inefficient operations are often imposed on DGs. Instabilities in the supply are taking place both in terms of rapid voltage and frequency fluctuations, but also as blackout occurrences, with each blackout lasting an average of more than 4 h. The sub-optimal exploitation of the generation asset in place in the MG is also exacerbated by the impossibility of injecting excess PV generation into the national grid due to Uganda's regulatory framework. The combined effect of the above-mentioned conditions results in high PV curtailment. A previous investigation on the same case study, devoted to optimally sizing the entire generation portfolio solely from an energetic point of view, can be found at [31]. Sizing a BESS to fully supply the MG is economically unfeasible due to the frequent occurrence of blackouts and the high magnitude of demand, which exceeds 200 kW.

Samples for frequency f_t and net load demand d_t are directly derived from the measurement campaign in [32]. Similarly, the hourly profiles are significant for a one-year period starting in April 2022. Employing a high-frequency sampling rate, a typical pattern of the hospital electric demand of the MG is captured: 100 s periodical and non-negligible load steps (30% of the average load) characterize the electric demand. Induced by the duty cycles of sterilizers, these fluctuations lead the rapid frequency oscillation during stand-alone operations, jeopardizing a reliable power dispatch.

In addition to real-world data gathering, key assumptions derived from the literature further support the analysis. The economic coefficients presented in Eqs. (4) and (5), listed in Table 2, are based on [33–35]. Given the vast availability of literature reporting numerical assumptions, the selected studies were included based on their affinity

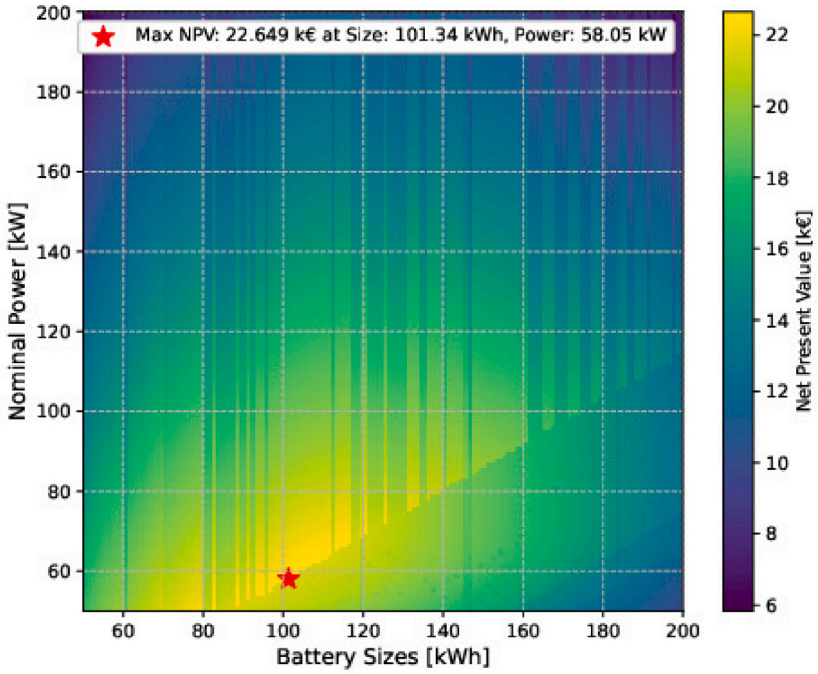

Fig. 5. NPV as a function of $E^{arbitrage}_{nom,BESS}$ and $P^{arbitrage}_{nom,BESS}$.

Table 3
Parameters' summary for DG governor.

Name	Type	Description	Range
T1	Seconds	Actuator time constant	0–25
T2	Seconds	Actuator time constant	0–0.5
T3	Seconds	Actuator time constant	0–10
T4	Seconds	Actuator time constant	0–25
T5	Seconds	Actuator time constant	0–10
T6	Seconds	Actuator time constant	0–0.5
T_d	Seconds	Engine delay	0–0.125
Droop	PU	Feedback gain	0–0.1
k	PU	Machine gain	15–25
T_e	Seconds	Power time constant	0–1
s	–	Switch droop control	0/1
J	kg m^2	Moment of inertia	7.2–10.8

with the case study and their relevance to MG applications in rural contexts within developing countries.

Regarding the tuning subsection of the methodology, the preprocessing phase involves the initial configuration of the heuristic search method proposed for DG characterization. Variability ranges for each time constant, provided in Table 3, are defined in accordance with technical standards [36]. Additionally, for the generator's physical inertia, a variation of 15% from the nominal inertia J is accepted. The operational hyper-parameters of the GA, introduced in Algorithm 2, are summarized in Table 4.

Result and discussion

BESS sizing for MG's energy support

The high penetration of PV generation and national grid unreliability certainly justify the presence of a BESS, aimed at smoothing the load supply. Given the mathematical framework presented in Section "Energy Sizing of the BESS", the annual, hourly discretized, economic-oriented BESS sizing resulted in a nominal BESS capacity of 101.3 kWh and a nominal power of 58 kW. Fig. 5 locates the least-cost solution for the yearly dispatch simulation by evaluating the NPV of possible combinations of capacity and nominal power. Battery size becomes more economically impactful due to its higher specific cost relative to nominal power capabilities. Additionally, a non-monotonous trend emerges due to the stochastic nature of load and PV generation. While larger battery sizes can reduce curtailment, the resulting operational improvements may have a minimal economic effect. Furthermore, a correlation between battery size and nominal power is evident: maximum benefits are achieved when both parameters are increased, as this ensures greater storage capacity and enables more effective utilization. However, battery energy storage systems with high energy-to-power ratios prove economically unviable due to the high electrical demand of the MG.

The limited-size BESS is designed to reduce curtailment, alleviate DG ramping during demand mismatches, and enhance the MG's resilience to sudden off-grid transitions. The MG's simulated dispatch over a five-day horizon, using the control rule detailed in Algorithm 1, is shown in Fig. 6. Due to its limited size, the BESS discharge occurs over a short period (marked by the red areas), sufficient to transition the system optimally to an off-grid configuration. Despite the BESS's constrained energy capacity, it, along with the PV plant's nominal output, helps avoid more than 50% of potential curtailment. A clear daily trend emerges: the peak load around midday is almost entirely covered by solar energy, while the grid provides power during off-peak hours and at night. However, some curtailment still occurs when there is a production surplus and the BESS is fully charged (as seen on the left side of Fig. 6). The BESS's role during blackouts is also evident: during the gray areas (when demand is met by the DG without the grid), the BESS discharges to optimally manage the DG, ensuring a smooth transition to off-grid operation and minimizing interruptions.

Table 4
Genetic algorithm parameters.

Parameter	Crossover	Selection	Mutation	Initial pop.	Iterations	Penalty function weight
Value	1	1	$\frac{1}{\sqrt{\text{It}}}$	40	30	1

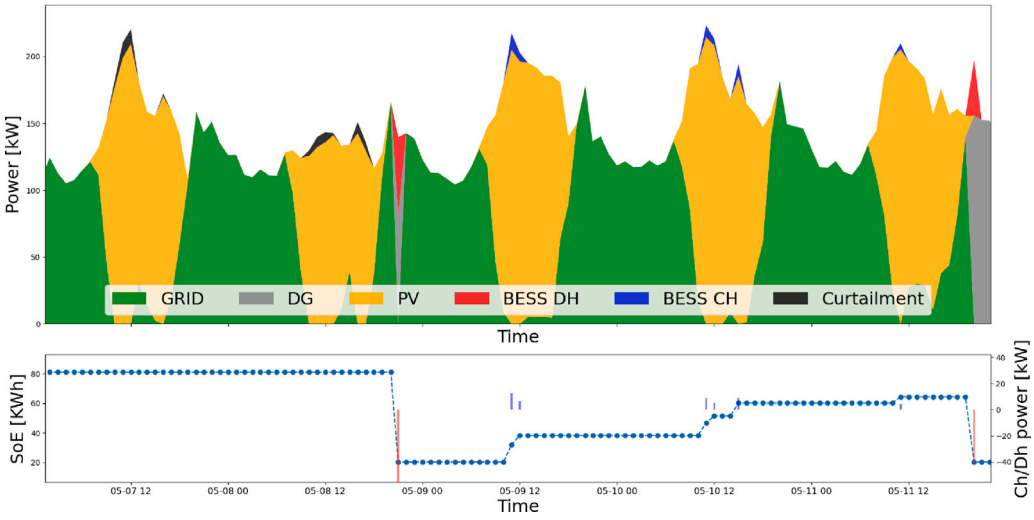

Fig. 6. Power dispatch of the MG and State of Energy (SoE) evolution in time. (For interpretation of the references to color in this figure legend, the reader is referred to the web version of this article.)

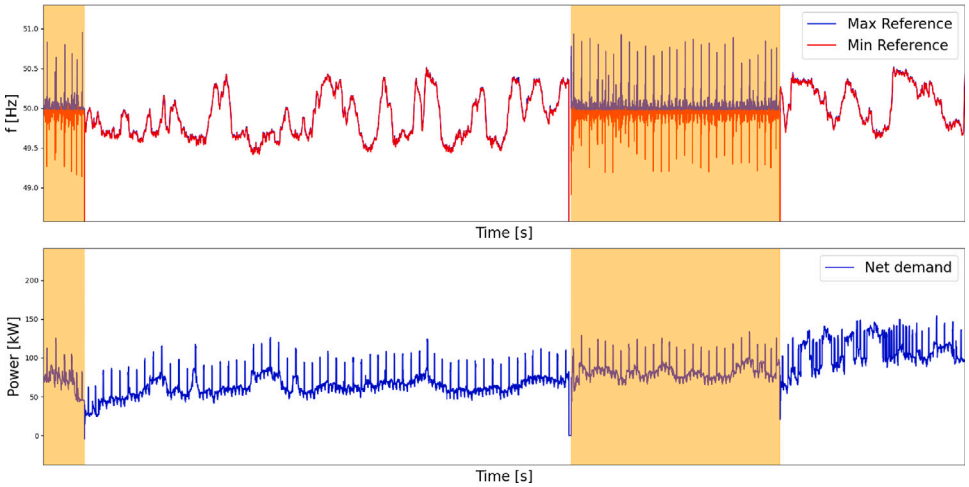

Fig. 7. Off-grid detection procedure applied on input power and frequency profiles. (For interpretation of the references to color in this figure legend, the reader is referred to the web version of this article.)

BESS sizing for MG's stability support

Energy-oriented battery sizing methodologies, typically employing low granularity data (e.g., hourly-based) for power dispatch, represent a pivotal yet incomplete step in the BESS sizing process for MGs.

Input data preparation and parameter initialization

Identifying off-grid segments is essential for characterizing the system's dynamic behavior. To achieve this, real-world data from the MG under study are used. The detection procedure identifies the occurrences and durations of main grid failures, during which the MG operates in islanded mode.

An increase in frequency fluctuations, particularly the RoCoF, serves as a clear indicator of islanded operations. As shown in the top part of Fig. 7, the variability in the minimum and maximum frequency references is used to identify off-grid segments, which are highlighted in yellow. The corresponding demand for these segments is isolated in the bottom graph. At this point, the off-grid records database in Fig. 4 is populated with segments that are sufficiently long, representative of MG trends, and evenly distributed across the input frequency records shown in Section "Data Gathering and Data Processing".

Governor tuning procedure

As described in Section "Stability constraints in sizing the BESS", the iterative framework within which the GA operates aims to progressively narrow down the range of variation for each parameter, facilitating optimal tuning.

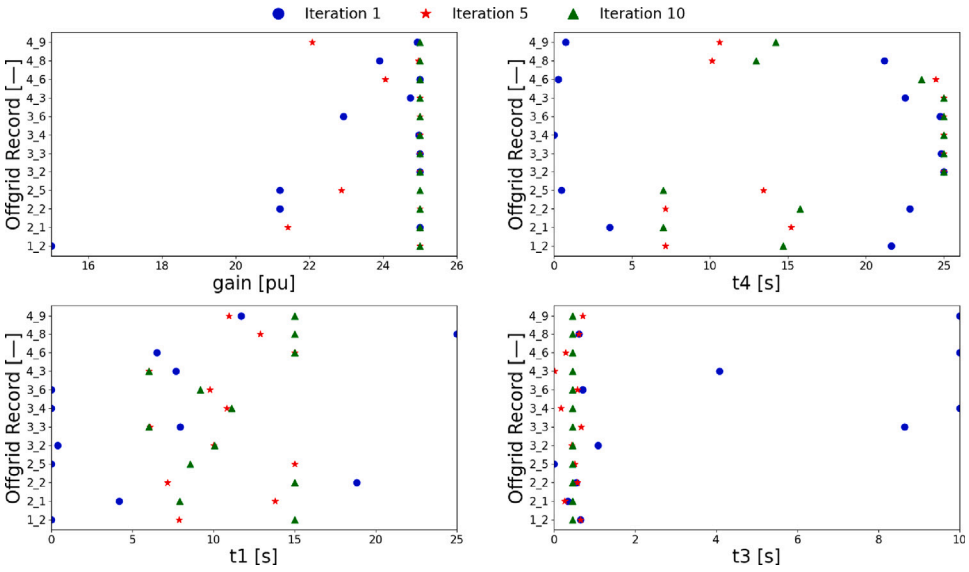

Fig. 8. Comparative results for transition between subsequent iterations.

The initial parameters and their corresponding variability ranges, presented in Table 3, are used as inputs for the genetic tuning process described in Section "Genetic Algorithm-Based Tuning for DG Governor Characterization". The results of subsequent iterations for the most relevant parameters are shown in Fig. 8, where the optimal estimations for each parameter are reported for every tuning procedure applied to each off-grid record. Several important observations emerge: first, a significant outcome arises from the shared isochronous regulation, resulting from the droop parameter estimations. This aligns with the expected behavior of the MG when operating off-grid, being the system powered by a single DG. As illustrated in the control schematic in Fig. 2a, this directly influences the relevance of other parameters, such as t_e and s, which become less significant in the dynamic response. Consequently, these parameters are excluded from the subsequent genetic search iterations. Second, the termination criterion is met for the parameters J, T_d, $T6$, and $T2$. Additionally, the variability ranges for the gain k and $T3$ are skewed toward their respective upper and lower bounds. This is particularly evident in the lower-right section of Fig. 8 for $T3$, where the limited degrees of freedom in the solution cause the variability of the remaining controllable parameters to shrink

In parallel, $t1$ and $t4$ mutually affect each other, and reaching a termination criterion becomes challenging. Consequently, a numerical sensitivity analysis was performed at this point to tune the last two parameters. The variability ranges were deeply investigated, relying on the reduced-order control block of Eq. (12): changes in the parameters directly affect the reciprocal position of poles and zeros impacting transient response in terms of overshooting and delay. Notably, $G(s)$ adjusts the power set point based on frequency deviation. In Fig. 9, the solution with T1 = 6 and T4 = 25 yields the maximum power set point for the same demand mismatch, resulting in the minimum frequency divergence.

$$G(s) = \frac{k \cdot (s \cdot T3 + 1)(s \cdot T4 + 1)}{s \cdot (s \cdot T1 + 1)} \tag{12}$$

The effectiveness of the developed procedure is evidenced by the evolution of the loss function, as depicted in Fig. 10. In particular, subsequent iterations demonstrate a consistent decrease in the loss function value concerning the initial iteration, indicative of the effectiveness of the combination of the GA and termination loop in converging towards the optimal set of parameters to characterize the dynamic response. A further consideration regards the loss function value at the final iteration in each simulation. The GA-based procedure yields a set of parameters that generate an acceptable dynamic response relative to the measured values. However, these results are achieved with varied, non-consensual values across different off-grid samples. Having a comparable value of loss function for the final iteration is in line with expectations. Indeed, the developed methodology is designed to derive a unified set of parameters capable of producing an optimal dynamic response across all considered off-grid frequency records.

The final optimal set of parameters is shown in Table 5. The top graph in Fig. 11 illustrates the frequency oscillations of the MG (in blue) with the optimal parameters, compared to the measured field frequency (in red). The simulated frequency closely matches the field measurements, suggesting a high-fidelity governor model. As expected, larger oscillations correspond to significant load changes, which can be seen in the bottom graph of Table 5. Two pivotal considerations are essential to correctly interpret these results. First, field measurements inherently include uncertainties from other frequency restoration mechanisms, which are now encapsulated in the governor's parameter values. In other words, while the governor's tuned parameters may differ from the real system's, they now account for these additional mechanisms and allow accurate replication of real-world fluctuations. Second, although application-specific, the model tends to overestimate frequency peaks, supporting conservative sizing: wider frequency oscillations demand a higher BESS peak capacity for stability services. Overall, the optimal governor parameters provide a reliable and robust replication of the MG's off-grid behavior. This allows, even in the absence of new field measurements, the simulation of scenarios such as the integration of additional generating assets (e.g., increased PV nominal power) and the assessment of the transient response of the low-inertia system to rapid demand changes, thereby identifying potential stability criticalities in advance.

Transient stability analysis with BESS

BESS's effectiveness in regulating frequency oscillation is tested and verified in Fig. 12: a 200 s time window, capturing two duty cycles of the sterilizer, was simulated, progressively increasing the power capability (10 kW, 20 kW, 30 kW) of the BESS to contribute to

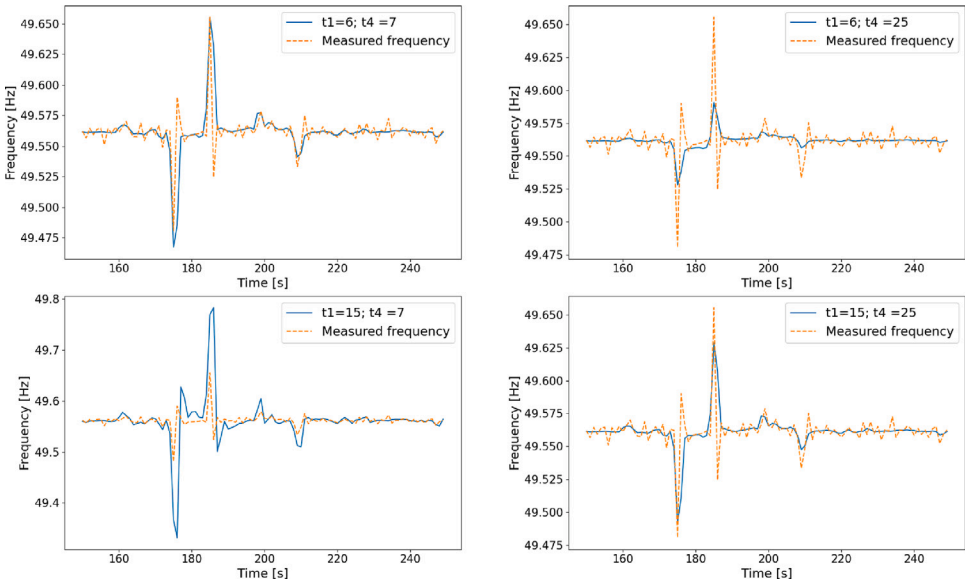

Fig. 9. Variability range exploration for t1 and t4.

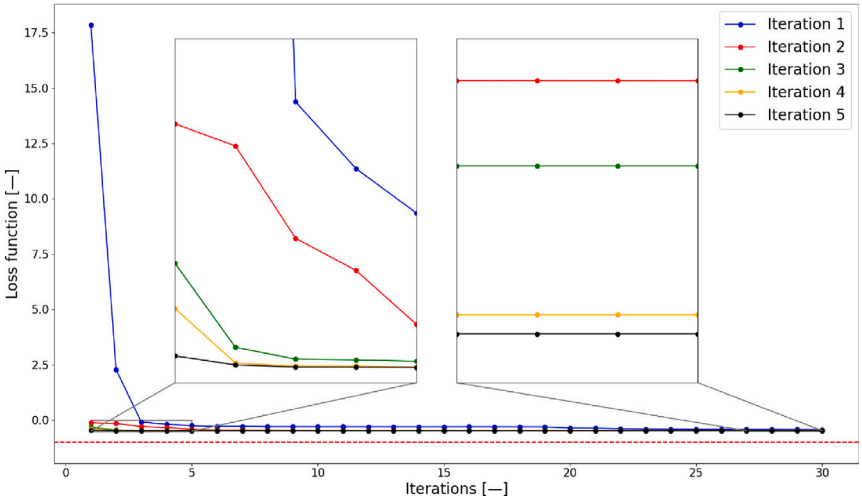

Fig. 10. Fitness value evolution for subsequent iterations.

stability. BESS sizes represent a fictitious power capacity of the asset to install fully devoted to frequency control; practically, the resulting size corresponds to a tentative for $\Delta P_{BESS}^{stability}$, concerning the definition of Fig. 1, and contribute to limit frequency deviation. Frequency control droop and deadband are selected as suggested in the literature for small MG application [10,32,37,38]: specifically, to identify operational limits, sensitivity analysis is performed keeping the droop coefficient K_p constant to 2%. Deadband is fixed to $\pm$0.01 p.u. concerning nominal frequency. Droop stability analysis using a small-signal state space model of the MG falls beyond the scope of the work representing a further step towards the real-life management of the MG. Generally speaking, droop control impacts the system performance: high gains reduce the stability margin while low gains make the MG less responsive with poor transient behaviors. Therefore, the selection of the droop is a trade-off between stability margin and dynamic performances [39].

Fig. 12 (upper section) shows the simulated frequency oscillations of the MG under the same load conditions while progressively increasing the BESS power capability. The corresponding time series of BESS power provision is reported in the lower section. Several key considerations arise when analyzing system performance under varying BESS power capabilities. Firstly, lower flexibility bands result saturated for wide load oscillations. As visible in the lower graph of Fig. 12, demand mismatch is not fully damped given the limited power availability and a plateau is reached for the 10 kW BESS. Conversely, the superposition of trends for higher power sizes (20 kW and 30 kW) suggests that frequency oscillations are not severe enough to fully exploit the BESS capability. Secondly, recalling demand fluctuation magnitude in Fig. 7, a flexibility band of 40 kW, resulting as the maximum fast load variation, is tested. Numeric results in Table 6 show a reduced marginal impact of a higher flexibility band. Not the entire share of a sudden load change is in charge of the BESS, as a result of the complex interaction of system inertia and DG's regulating capabilities. Based on these findings, the range of 10–20 kW was identified as providing effective frequency support for the MG, given the load patterns and intermittent operation of appliances. To ensure a reliable cost estimation, the nominal stability power requirement of the BESS, $\Delta P_{nom,BESS}^{stability}$, was conservatively set at 20 kW. As previously mentioned, given the MG under investigation, the human operator must assess the optimal trade-off between performance improvement and cost increase.

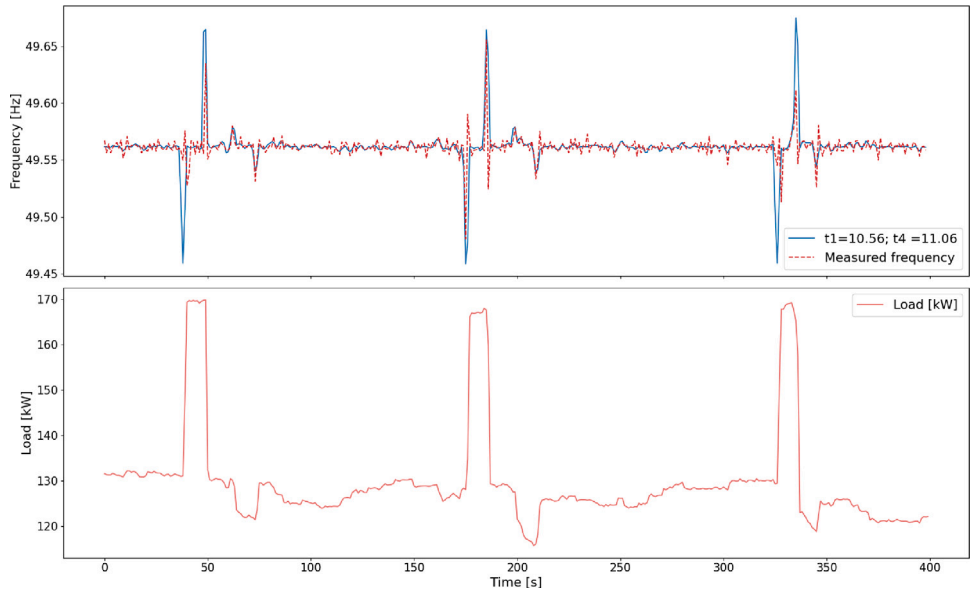

Fig. 11. Measured and simulated frequency oscillation in response to the same load demand. (For interpretation of the references to color in this figure legend, the reader is referred to the web version of this article.)

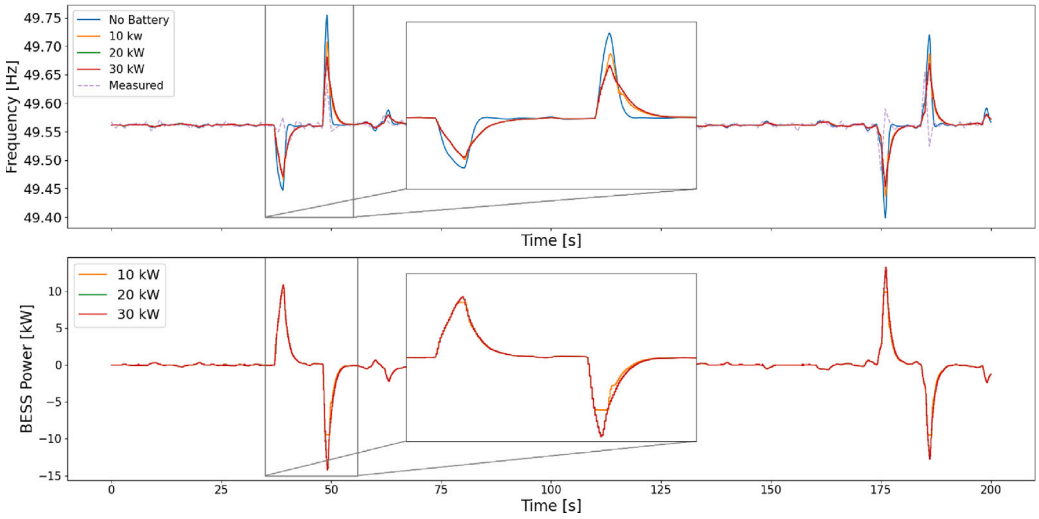

Fig. 12. Simulated frequency and power for different BESS sizes.

Multi criteria BESS numeric sizing

Given the sterilizer's duty cycle, in the Lacor Hospital case study, CF is assumed unitary, indicating the high probability of simultaneously exploiting the two services. On the other hand, PFC was demonstrated to be a balanced, power-intensive service, with power interactions, although significant, restricted to short periods of charging and discharging the BESS. To support this last consideration, the energy contribution ΔE, reported in Table 6, demonstrates the limited energetic impact of the stability services. Beside the sign of the variation, that is case sensitive, the impact is limited below 0.1% of the BESS size. As a result of all previous considerations and considering that BESS is not expected to fully and continuously supply its load when off grid, $\Delta E^{stability}_{nom,BESS}$, is set to 0 kWh.

Comparing the optimal configuration with the existing setup of the MG, the integration of the BESS yields significant benefits. From an energetic perspective, the BESS reduces DG consumption and curtailed energy by 11.1% and 42.9%, respectively, with a total annual energy throughput of 5.5 MWh. These results align with the dispatch profiles in Fig. 6, where BESS operation (blue areas) largely replaces curtailed energy (black areas). In terms of stability, the BESS provides substantial improvements, achieving a 64.1% reduction in peak-to-peak frequency oscillations, as quantitatively reported in Table 6. Economically, the total cost of the BESS is estimated at 26.7 k€, with 6.2% of this cost attributed to its stability services. Additionally, yearly savings from reduced fuel consumption and DG OPEX amount to 1.2 k€. Additionally, a strong benefit is supposed to be achieved in terms of power quality and reliability of the energy supply.

Overall, the strong agreement with field measurements and the integration of transient stability considerations make the proposed method a credible and practically applicable tool for BESS sizing in

Table 5
Optimal parameters for the DG's governor.

Name	T1	T2	T3	T4	T5	T6	T_d	Droop	k	T_e	s	J
Opt. Val.	10.56	0	0.45	11.06	0	0	0	0	25	0	0	9.58

Table 6
Frequency reference quantities.

	Nadir [Hz]	Zenith [Hz]	ROCOF [Hz/s]	ΔE [%]
No battery	49.398	49.76	0.29	
10 kW	49.436	49.71	0.19	0.088
20 kW	49.47	49.65	0.17	0.077
30 kW	49.49	49.62	0.16	0.072
40 kW	49.49	49.62	0.16	0.072

MGs, complementing and extending existing approaches in the literature. Specifically, compared to conventional metaheuristic approaches reported in the literature (e.g., particle swarm optimization [11] or optimization model [10,40]), the proposed real-coded genetic algorithm is specifically tailored for MG frequency response modeling, reducing the computational effort while maintaining high accuracy. Furthermore, unlike most existing studies that focus solely on steady-state adequacy [17], the present method integrates transient stability analysis, providing a more holistic framework for BESS sizing.

Conclusions

This research presents an integrated adequacy and stability sizing methodology for BESS in PV-based MGs, specifically designed for developing countries. The present methodology supports the entire sizing process by evaluating BESS as a key asset for enhancing system stability, defined as the ability to operate closer to 50 Hz, and reliability, defined as the capacity to manage faults and disturbances. A key challenge identified in the literature is the economic feasibility of high self-consumption levels and complete DG phase-out, which requires significant upfront investment. Additionally, the role of BESS in stabilizing MG dynamics is often constrained by data scarcity and the unreliable characterization of DG behavior.

To overcome these limitations, the proposed methodology employs a real-coded genetic algorithm that integrates real-world measurement-based data with numerical sizing procedures. Despite multiple uncertainty sources, this hybrid approach ensures that both energetic adequacy and stability considerations are optimally addressed. The effectiveness of the method was demonstrated through its application to the MG of Lacor Hospital in Uganda. An iterative tuning of the governor was conducted using 12 off-grid samples to accurately reconstruct the system's dynamic behavior. Dynamic simulations identified a stability service requirement of 10–20 kW, with the final sizing conservatively set at 20 kW. Energetic adequacy was ensured through a rule-based control logic that reflects real-world conditions, resulting in a 101.34 kWh, 78.05 kW BESS at a total cost of €26.7k, of which 6.2% was allocated to stability functions. The approach led to a 42% reduction in yearly energy curtailment and a 64.1% reduction in frequency peak-to-peak variability.

While the results obtained for Lacor Hospital demonstrate the effectiveness of the proposed methodology, certain limitations must be acknowledged. The economic feasibility assessment relies on numerical assumptions that do not account for price fluctuations in BESS technology. Future research should include sensitivity analyses to evaluate the impact of cost variations and improve the robustness of financial assessments. Additionally, the nonlinear nature of the sizing problem suggests the need for more advanced metaheuristic techniques to enhance computational efficiency and scalability. Further improvements can be made by testing the methodology across diverse case studies with varying load characteristics to assess its generalizability. Data collection also presents a limitation, as higher-frequency records (e.g., one-second sampled profiles of frequency and demand) over extended time periods would capture seasonal variations, thereby improving governor characterization. Expanding this approach to other MGs underscores the critical need for an integrated methodology that simultaneously addresses energy adequacy and stability in off-grid MGs. In regions with poor energy security and low-inertia systems, combining energy arbitrage with power stability within a unified framework is essential. This would allow for more accurate economic assessments and ensure systems are optimally sized and planned to meet real-life challenges, balancing efficient energy management with grid reliability.

CRediT authorship contribution statement

Corrado Maria Caminiti: Writing – review & editing, Writing – original draft, Visualization, Validation, Software, Resources, Methodology, Investigation, Formal analysis, Data curation, Conceptualization. **Matteo Spiller:** Writing – review & editing, Writing – original draft, Software, Methodology, Conceptualization. **Aleksandar Dimovski:** Writing – review & editing, Writing – original draft, Supervision, Methodology, Conceptualization. **Jacopo Barbieri:** Writing – review & editing, Supervision, Data curation, Conceptualization. **Enrico Ragaini:** Writing – review & editing, Supervision, Data curation, Conceptualization. **Marco Merlo:** Writing – review & editing, Writing – original draft, Supervision, Resources, Project administration, Methodology, Formal analysis, Data curation, Conceptualization.

Declaration of competing interest

The authors declare that they have no known competing financial interests or personal relationships that could have appeared to influence the work reported in this paper.

Acknowledgment

Corrado Maria Caminiti scholarship is funded by ABB Italy.

Appendix. Supplementary data

A.1. Algorithms

Algorithm 1 Control logic of the MG power dispatch

t in T are the hourly timeframes of a year
▷ Input:
P_t^{load} is the electric load demand in kW, P_t^{PV} is the PV generation in kW
AV_t is the binary grid availability in each timeframe
▷ Auxiliary variables:
P_t^{net} is the net demand P_t^{load} - P_t^{PV}
▷ Variables:
P_t^{DG} is the power supplied by DG in kW
$P_t^{ch,BESS}$ and $P_t^{dh,BESS}$ are the power interactions with the BESS in kW
for $E_{nom,BESS}^{arbitrage}$ and $P_{nom,BESS}^{arbitrage}$ in ranges: **do**
  for t in T: **do**
    if AV_t **then**
      if $P_t^{net} > 0$ **then**
        Supply with the grid power
      else
        Store the over generation in the battery ($P_t^{ch,BESS}$)
        Curtail the excess with respect to $E_{nom,BESS}$ or $P_{nom,BESS}^{arbitrage}$
      end if
      Supply the load with the stored energy in BESS ($P_t^{dh,BESS}$)
      DG follows (P_t^{DG})
    end if
  end for
end for

Algorithm 2 Genetic Algorithm metacode

```
Initial population set up with parameters in Table 3 as thresholds.
New_population ← initial_population
                                                    ▷ Simulation section:
for iteration in Iterations do
    for individual in New_population do
        Run an RMS simulation
        Compute the objective function
    end for
    Sort the population by the objective function
    Store the results
                                                    ▷ Selection section:
    for each individual in Next_population do
        for parameter in Parameters do
            if random number < p_crossover then
                New offspring = Crossover procedure
            end if
            if random number < p_mutation then
                New parameter ← {normal, Cauchy or Lévy distribution}
            end if
        end for
    end for
    New_population ← New offspring, New parameter
end for
```

Data availability

Data will be made available on request.

References

[1] IEA. World energy outlook 2023. Paris: IEA; 2023, https://www.iea.org/reports/world-energy-outlook-2023, licence: CC bY 4.0 (report); CC bY NC sA 4.0, Annex A.

[2] IEA, IRENA, UNSD, World Bank, WHO. Tracking SDG 7: The energy progress report. Washington DC: World Bank; 2023, © World Bank. License: Creative Commons Attribution—NonCommercial 3.0 IGO (CC BY-NC 3.0 IGO).

[3] Al-falahi MD, Jayasinghe S, Enshaei H. A review on recent size optimization methodologies for standalone solar and wind hybrid renewable energy system. Energy Convers Manage 2017;143:252–74. http://dx.doi.org/10.1016/j.enconman.2017.04.019.

[4] Mathew M, Hossain MS, Saha S, Mondal S, Haque ME. Sizing approaches for solar photovoltaic-based microgrids: A comprehensive review. IET Energy Syst Integr 2022;4(1):1–27. http://dx.doi.org/10.1049/esi2.12048.

[5] Felice A, Barbieri J, Martinez Alonso A, Messagie M, Coosemans T. Challenges of phasing out emergency diesel generators: The case study of lacor hospital's energy community. Energies 2023;16. http://dx.doi.org/10.3390/en16031369.

[6] Bonkile MP, Ramadesigan V. Effects of sizing on battery life and generation cost in PV–wind battery hybrid systems. J Clean Prod 2022;340:130341. http://dx.doi.org/10.1016/j.jclepro.2021.130341.

[7] Jamali A, Nor NM, Ibrahim T. Energy storage systems and their sizing techniques in power system — A review. In: 2015 IEEE conference on energy conversion. CENCON, 2015, p. 215–20. http://dx.doi.org/10.1109/CENCON.2015.7409542.

[8] Khatib T, Ibrahim IA, Mohamed A. A review on sizing methodologies of photovoltaic array and storage battery in a standalone photovoltaic system. Energy Convers Manage 2016;120:430–48. http://dx.doi.org/10.1016/j.enconman.2016.05.011.

[9] Saeed MH, Fangzong W, Kalwar BA, Iqbal S. A review on microgrids' challenges and perspectives. IEEE Access 2021;9:166502–17. http://dx.doi.org/10.1109/ACCESS.2021.3135083.

[10] Javadi M, Gong Y, Chung CY. Frequency stability constrained BESS sizing model for microgrids. IEEE Trans Power Syst 2024;39(2):2866–78. http://dx.doi.org/10.1109/TPWRS.2023.3284854.

[11] El-Bidairi KS, Nguyen HD, Mahmoud TS, Jayasinghe S, Guerrero JM. Optimal sizing of battery energy storage systems for dynamic frequency control in an islanded microgrid: A case study of Flinders Island, Australia. Energy 2020;195:117059. http://dx.doi.org/10.1016/j.energy.2020.117059.

[12] Asad M, Martinez S, Sanchez-Fernandez JA. Diesel governor tuning for isolated hybrid power systems. Electronics 2023;12(11). http://dx.doi.org/10.3390/electronics12112487.

[13] Lin C-H, Wu C-J, Yang J-Z, Liao C-J. Parameters identification of reduced governor system model for diesel-engine generator by using hybrid particle swarm optimisation. IET Electr Power Appl 2018;12(9):1265–71. http://dx.doi.org/10.1049/iet-epa.2017.0851.

[14] Shah C, Wies RW, Hansen TM, Tonkoski R, Shirazi M, Cicilio P. High-fidelity model of stand-alone diesel electric generator with hybrid turbine-governor configuration for microgrid studies. IEEE Access 2022;10:110537–47. http://dx.doi.org/10.1109/ACCESS.2022.3211300.

[15] Zaker B, Gharehpetian GB, Karrari M. A novel measurement-based dynamic equivalent model of grid-connected microgrids. IEEE Trans Ind Inform 2019;15(4):2032–43. http://dx.doi.org/10.1109/TII.2018.2856852.

[16] Patel H, Chowdhury S. Review of technical and economic challenges for implementing rural microgrids in South Africa. In: 2015 IEEE eindhoven powerTech. 2015, p. 1–6. http://dx.doi.org/10.1109/PTC.2015.7232341.

[17] Gebrehiwot K, Mondal MAH, Ringler C, Gebremeskel AG. Optimization and cost-benefit assessment of hybrid power systems for off-grid rural electrification in Ethiopia. Energy 2019;177:234–46. http://dx.doi.org/10.1016/j.energy.2019.04.095.

[18] Islam MR, Akter H, Howlader HOR, Senjyu T. Optimal sizing and techno-economic analysis of grid-independent hybrid energy system for sustained rural electrification in developing countries: A case study in Bangladesh. Energies 2022;15(17). http://dx.doi.org/10.3390/en15176381.

[19] Aziz AS, Tajuddin MFN, Adzman MR, Mohammed MF, Ramli MA. Feasibility analysis of grid-connected and islanded operation of a solar PV microgrid system: A case study of Iraq. Energy 2020;191:116591. http://dx.doi.org/10.1016/j.energy.2019.116591.

[20] Hosseini ZS, Khodaei A, Paaso EA, Hossan MS, Lelic D. Dynamic solar hosting capacity calculations in microgrids. 2018, arXiv:1809.10133.

[21] Pfenninger S, DeCarolis J, Hirth L, Quoilin S, Staffell I. The importance of open data and software: Is energy research lagging behind? Energy Policy 2017;101:211–5. http://dx.doi.org/10.1016/j.enpol.2016.11.046.

[22] Makolo P, Oladeji I, Zamora R, Lie T-T. Data-driven inertia estimation based on frequency gradient for power systems with high penetration of renewable energy sources. Electr Power Syst Res 2021;195:107171. http://dx.doi.org/10.1016/j.epsr.2021.107171.

[23] Stefopoulos G, Georgilakis P, Hatziargyriou N, Sakis Meliopoulos A. A genetic algorithm solution to the governor-turbine dynamic model identification in multi-machine power systems. In: Proceedings of the 44th IEEE conference on decision and control. 2005, p. 1288–94. http://dx.doi.org/10.1109/CDC.2005.1582336.

[24] Daccò E, Falabretti D, Vicario A. Intentional islanding of active distribution networks by GenSets: An analysis of technical constraints and opportunities. Int Trans Electr Energy Syst 2023;2023(1):3048966. http://dx.doi.org/10.1155/2023/3048966.

[25] Wang J, Zhang M, Ersoy OK, Sun K, Bi Y. An improved real-coded genetic algorithm using the heuristical normal distribution and direction-based crossover. Comput Intell Neurosci 2019;2019(1):4243853. http://dx.doi.org/10.1155/2019/4243853, arXiv:https://onlinelibrary.wiley.com/doi/pdf/10.1155/2019/4243853.

[26] Rommes J, Martins N, Freitas FD. Computing rightmost eigenvalues for small-signal stability assessment of large-scale power systems. IEEE Trans Power Syst 2010;25(2):929–38. http://dx.doi.org/10.1109/TPWRS.2009.2036822.

[27] Wang J, Song Y, Hill DJ, Liu T. Microgrid stability enhancement by incorporating BESS droop gain tuning. In: 2021 IEEE PES innovative smart grid technologies Europe. ISGT Europe, 2021, p. 1–5. http://dx.doi.org/10.1109/ISGTEurope52324.2021.9640181.

[28] Spiller M, Vicario A, Rancilio G, Dimovski A, Palamara G, Merlo M. Impact of BESS frequency control on microgrids: the case study of the small Island Lipari. In: 2023 international conference on electrical, computer and energy technologies. ICECET, 2023, p. 1–6. http://dx.doi.org/10.1109/ICECET58911.2023.10389579.

[29] Rancilio G, Vicario A, Merlo M, Berizzi A. 6 - battery energy storage contribution to system frequency for grids with high renewable energy sources penetration. In: Mishra DK, Li L, Zhang J, Hossain MJ, editors. Power system frequency control. Academic Press; 2023, p. 133–50. http://dx.doi.org/10.1016/B978-0-443-18426-0.00005-4.

[30] Fondazione Corti LH. Values and mission. 2024, URL https://fondazionecorti.it/en/lacor-hospital/.

[31] Bosisio A, Moncecchi M, Cassetti G, Merlo M. Microgrid design and operation for sensible loads: Lacor hospital case study in Uganda. Sustain Energy Technol Assess 2019;36:100535. http://dx.doi.org/10.1016/j.seta.2019.100535.

[32] Dimovski A, Ragaini E, Barbieri J, Sangiorgio I, Albertini LMF, Aghahadi M, Mauri M, Mereu R, Merlo M. The role of digitalization in planning and operation of microgrids in emerging countries. In: 2023 international conference on clean electrical power. ICCEP, 2023, p. 546–53. http://dx.doi.org/10.1109/ICCEP57914.2023.10247387.

[33] Petrelli M, Fioriti D, Berizzi A, Poli D. Multi-year planning of a rural microgrid considering storage degradation. IEEE Trans Power Syst 2021;36:1459–69. http://dx.doi.org/10.1109/TPWRS.2020.3020219.

[34] Solano-Peralta M, Moner-Girona M, van Sark W, Vallve X. "Tropicalisation" of Feed-in Tariffs: A custom-made support scheme for hybrid PV/diesel systems in isolated regions. Renew Sustain Energy Rev 2009;13:2279–94. http://dx.doi.org/10.1016/j.rser.2009.06.022.

[35] Nebuloni R, Meraldi L, Moretti L, Ilea V, Bovo C, Berizzi A, Raboni P. A real-time cycle counting method for battery degradation calculation in MILP models. In: 2023 IEEE international conference on environment and electrical engineering and 2023 IEEE industrial and commercial power systems Europe. 2023, p. 1–6. http://dx.doi.org/10.1109/EEEIC/ICPSEurope57605.2023.10194776.

[36] NEPLAN. Turbine-governor models: Standard dynamic turbine-governor systems in NEPLAN power system analysis tool. Küsnacht, Switzerland: NEPLAN AG; 2024, © NEPLAN AG. All rights reserved..

[37] Abayateye J, Corigliano S, Merlo M, Zimmerle D. BESS primary frequency control strategies for the West Africa power pool. Energies 2022;15(3). http://dx.doi.org/10.3390/en15030990.

[38] Betancourt OA, Sanchez Z, Saleh S, Hill E, Zhao X, Sanchez F. Battery energy storage systems for primary frequency regulation in island power systems. In: 2020 IEEE/IAS 56th industrial and commercial power systems technical conference. ICPS, 2020, p. 1–10. http://dx.doi.org/10.1109/ICPS48389.2020.9176784.

[39] Barklund E, Pogaku N, Prodanovic M, Hernandez-Aramburo C, Green TC. Energy management in autonomous microgrid using stability-constrained droop control of inverters. IEEE Trans Power Electron 2008;23(5):2346–52. http://dx.doi.org/10.1109/TPEL.2008.2001910.

[40] Wu X, Zhao J, Conejo AJ. Optimal battery sizing for frequency regulation and energy arbitrage. IEEE Trans Power Deliv 2022;37(3):2016–23. http://dx.doi.org/10.1109/TPWRD.2021.3102420.